LQG/LTR ROBUST SEMI-ACTIVE SUSPENSION CONTROL SYSTEM USING MAGNETO-RHEOLOGICAL DAMPERS

Claudio Crivellaro, e-mail: claudio.crivellaro@metalsa.com
Metalsa Brasil

Decio Crisol Donha, e-mail: decdonha@usp.br
Mechanical Department of Polytechnic School University of São Paulo

Abstract. *This work presents the complete design of a semi-active suspension control system for a Sport Utility Vehicle (SUV). The main control objective is the performance improvement in comfort and safety features of the vehicle. The design is based on a LQG/LTR robust control strategy for non-strictly proper system, using a full dynamic model with seven degrees of freedom. Magneto-rheological dampers prototypes were designed and used as actuators and sensors with costs compatible to the application were employed. Results from simulations and experimental trials are presented and analyzed, showing that the proposed control system was able to improve the comfort and safety performances, avoiding the loss of adherence between tyres and the ground and other undesirable dynamic behaviors of the vehicle .*

Keywords*: pickup suspension, magneto-rheological dampers, robust control, LQG/LTR, semi-active suspension*

1. INTRODUCTION

This work presents the complete development of a semi-active suspension prototype for a Sport Utility Vehicle (SUV). The development was two folded. The first part of the work dealt with the development of a magneto-rheological damper, able to control the movements of a pick-up suspension. A first result here was the construction of a damper prototype with a very good performance, which was applied in a real vehicle, in this case, a Ford Ranger pick-up.

The second part of the work consisted of the implementation and test of the semi-active suspension. To reach this goal, at first a control system was synthesized using a sophisticated control strategy based on the Linear Quadratic Gaussian/ Loop Transfer Recovery (LQG/LTR) robust control approach, adapted to the semi-active condition. In practice, a control algorithm was implemented in a Digital Signal Processor (DSP), using the Matlab/Simulink software and the DSP target hardware. Next, the control system was implemented in the vehicle assembled with four magneto-rheological dampers. The semi-active suspension performance was then evaluated by the RMS values of pitch, roll and heave accelerations of the vehicle body during tests using disturbances generated by different road profiles. To evaluate the performance improvement, results obtained with the semi-active suspension were compared to results obtained with a passive suspension, where dampers with fixed damping function (non-linear damping curves) replaced the semi-active actuators.

2. SEMI-ACTIVE ACTUATOR DESIGN

In recent years, semi-active control devices have received significant attention because they can offer the adaptability of active control devices without requiring their associated large power sources. Magneto-rheological (MR) dampers are semi-active control devices that use MR fluids to produce controllable dampers. They potentially offer highly reliable operation and are viewed as fail-safe once that, in the case of malfunction, they become passive dampers.

Before to built the complete semi-active suspension, four MR dampers were designed following the practical design procedure described in Crivellaro and Santos (2004) and in volume 1 of Crivellaro (2008), where the “minimum active volume of fluid” concept and magneto-static finite element analysis (FEA) was used. The prototypes were built based on mono-tubular concept with a chamber of pressured air (about 15 bar). The bushings and joints had to be compatible to the pickup suspension assembly. These MR dampers were installed in a real vehicle, specifically a pickup truck Ford Ranger. The CAD 3D model of the frontal suspension damper is showed in Fig. 1, whereas Fig. 2 presents the prototypes of the dampers.

Figure 1. 3D model of magneto-rheological damper.

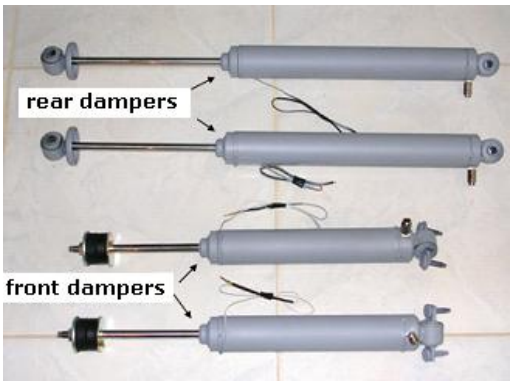

Figure 2. Magneto-rheological damper prototypes

As shown, four prototypes were built: two for the frontal pickup suspension, and two for the rear suspension. Obviously, the specifications included the dimensions (length, stroke, diameter, etc) of original Ranger pickup suspension dampers. Additionally, the MR damper controllable force should reach approximately 2600 N and a residual damper coefficient of 400 N.s/m was needed. Roughly speaking, this means that the MR damper force can change from a value lower than the minimum compression force of the original Ranger dampers to values higher than the maximum traction force of original dampers.

The prototypes were tested in a MTS equipment locate at Dana Nakata Test Labs as presented in Crivellaro and Alves (2006), and the results were very satisfactory, accomplishing specifications and reaching forces around 3 kN, enough to control a 1.5 ton pickup truck. Typical response curves of these prototypes are shown in Fig. 3.

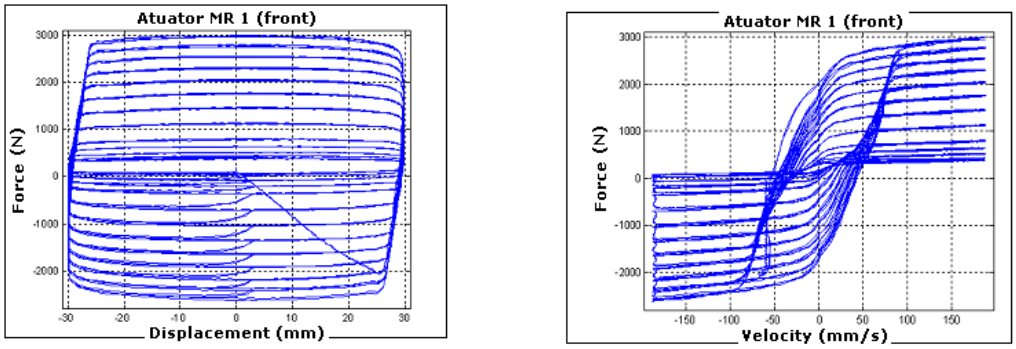

Figure 3. MR Dampers response curves.

In the graphs of Fig. 3 the different levels of force correspond to different levels of electric voltage (from 0.5 to 10 volts) in the damper control terminals.

Figure 4 shows the dampers installed in the vehicle. Despite the electric connections, the assembly is similar to the conventional damper setup.

Figure 4. MR dampers prototypes installed in the pickup Ford Ranger.

3. CONTROL SYNTHESIS

The aim of control synthesis shall be to find a Transfer Function Matrix (TFM) **K**(s) that improves the comfort of the vehicle, i. e., reduces the acceleration amplitude of vehicle suspended mass. As shown in Fig. 5, the control synthesis basically consists to calculate the matrices **H** and **G** using the LQG/LTR methodology. After this methodology, matrix **K**(s) can then be written as follows (Cruz, 1996):

$$\mathbf{K}(s) = -\mathbf{S_r} \cdot \mathbf{S_u} \cdot \mathbf{G} \cdot (s\mathbf{I} - \mathbf{A_b} + \mathbf{B_n} \cdot \mathbf{G} + \mathbf{H} \cdot \mathbf{C_b} - \mathbf{H} \cdot \mathbf{D_n} \cdot \mathbf{G})^{-1} \cdot \mathbf{H} \cdot \mathbf{S_r^T}$$

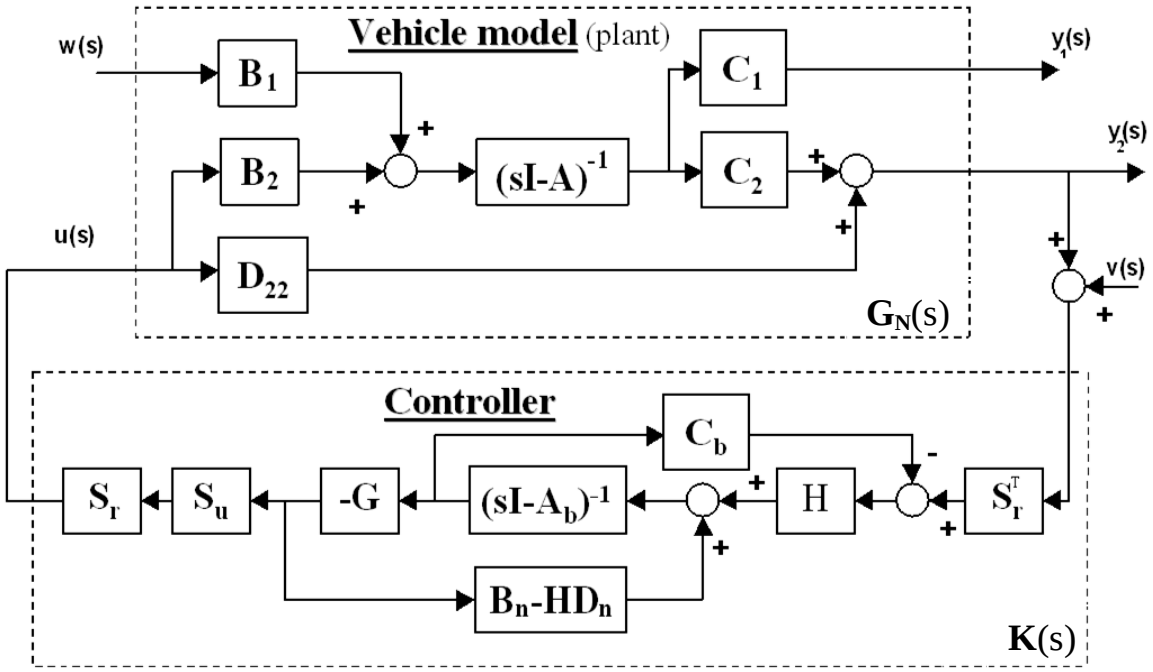

Figure 5. Block diagram of controlled suspension system.

Matrices **A**, **B**, **C** and **D** are given by the vehicle mathematical model. The complete procedure to identify these matrices can be found at Crivellaro and Donha (2011b). The numerical indexes of matrices presented in Fig. 5 indicate appropriate partition of the considered matrix. Index "b" and "n" stands for "balanced" and "normalized", respectively.

Using the LQG/LTR methodology, to guarantee robust control and desired levels of performance, a series of barriers are imposed to shape the singular values of the open loop multivariable function $\mathbf{G_N}(j\omega) \cdot \mathbf{K}(j\omega)$ (Crivellaro and Donha, 2011a). The first barrier imposed, $\mathbf{a_r}$, is associated with the physical limitations of the rattle-space. In active and semi-active suspension systems, it is necessary to impose an upper limit to the controller gain in frequencies below

0.5Hz, otherwise the amplitudes of the displacement of wheel relatively to the chassis may become too large. Since the rattle-space is obviously limited by construction constraints, the movement of the wheel and of the vehicle body may reach its mechanical limitation, producing shocks between elements and great discomfort. Furthermore, large control gains in the low frequency range are often associated to an operation of integration, which is not recommended for systems where the input signals for the controller is achieved by accelerometers. Accelerometers often present measurement bias, which integration leads to saturation of actuators.

Next, to guarantee a satisfactory disturbance rejection in the plant output and insensitivity to variations in plant parameters, it is introduced the barrier $\mathbf{a_c}$, also associated to the level of comfort for users. One way to easily qualify comfort is through the RMS of the acceleration imposed to the body of users, where the exposure time and the range of frequency are also important parameters. As it is well known, there are international standard norms classifying allowed vibrations for users of vehicles (e.g. ISO 2631-1 and SAE J1490). These norms indicate that the critical range of frequency vibration to the human body is roughly between 4 and 8 Hz in the vertical direction and 1 to 2 Hz for movements in the horizontal plane. Considering that the intensity of external disturbances and of the plant variations due to changes in the suspended mass are maximal between 1 and 8 Hz, barrier $\mathbf{a_c}$ is imposed in this frequency range as a lower limit, since the controller must provide a minimum level of actuation to counteract external disturbances and to face the problem of parameter variations of the plant. In other words, this barrier will guarantee disturbance rejection in this frequency range.

Another problem to be taken into account is the jerk, associated to comfort problems known as harshness and straightly connected to the sudden changes in the acceleration sense. Due to its way of construction and action, semi-active suspensions are prone to increase jerk, clearly deteriorating the comfort performance. Dampers in semi-active suspensions may only generate forces in one sense, producing forces discontinuously, once the damper can only produce dissipative forces against the relative motion. Vertical motions of the suspended and non-suspended masses are not always synchronized and usually have different frequency of oscillation. In this case, an active control action is needed. To minimize this kind of problem in semi-active suspensions, the controller simply switches of the actuator, generating discontinuities in the control force. Semi-active suspensions may still present discontinuity of action due to hysteresis imposed by a characteristic relationship of force and actuator velocity. Since control algorithms for semi-active suspensions usually switch the control signals exactly when the relative velocity is null, and in this situation the force is not null, there is always a sudden change of the force. Finally, jerk may also occur due to non-linearities of the suspension such as end courses, stops and elastic responses of tires to the shock with the road. Jerk is still a problem not totally solved in most semi-active suspensions. The third barrier to be imposed, barrier $\mathbf{a_j}$, is intended to set a n upper limit to the open-loop gain, reducing jerk indirectly and avoiding that a strong control action increases the lag between the relative velocity of the suspended and non-suspended masses and the vertical velocity of the suspended mass.

The fourth barrier to be imposed, $\mathbf{a_s}$, is intended to guarantee that the wheels do not lose contact with the road, improving in this way the safety performance. This barrier also set an upper limit to the open loop, now in the wheel-rope range, occurring between 9 and 12 Hz. If the controller tries to reduce the movements of the suspended mass in this frequency range, the amplitude of motions of the wheel tends to increase, producing a large oscillation of the contact force between the road and the wheel and reducing the adherence of the vehicle. The vibration amplitudes of the vehicle structure are significant for frequencies above of the resonance frequency of the non-suspended mass. Since these vibration modes are not modeled, the model error will rise in this frequency range when the controller is working with the real vehicle.

To diminish the influence of the model error a fifth barrier, $\mathbf{a_e}$, is added, leading the open loop gain to be limited by its maximum value in the range of frequencies between 30 Hz and 200 Hz.

At last, a sixth barrier, $\mathbf{a_m}$, is added to mitigate the measurement error. In reality, barriers $\mathbf{a_e}$ and $\mathbf{a_m}$ are equivalent to the barrier given. Although the system is described by an continuous system in time, the implementation of the real control system is made by an electronic circuit operating under time intervals, and the control action is actually discrete. In this case, the frequency of noise and errors is equal to the sampling rate from the signals of sensors. The objective of this barrier is to restrain the control gain to values bellow -30 dB, leading the own controller to work as a filter of sensor errors and noise.

The six barriers presented before are displaced in a Bode multivariable $\mathbf{G_N} \cdot \mathbf{K}$ graphic, as shown in Fig.6.

The next step in a LQG/LTR control design procedure would be to choose a controller $\mathbf{K}(s)$ so that the maximum singular value curve ($\bar{\sigma}(\mathbf{G_N}(j\omega) \cdot \mathbf{K}(j\omega))$ and the minimum singular value curve ($\underline{\sigma}(\mathbf{G_N}(j\omega) \cdot \mathbf{K}(j\omega))$ run between the barriers, as illustratively shows the blue curves in Fig. 6 (Skogestad and Postlethwaite, 1986).

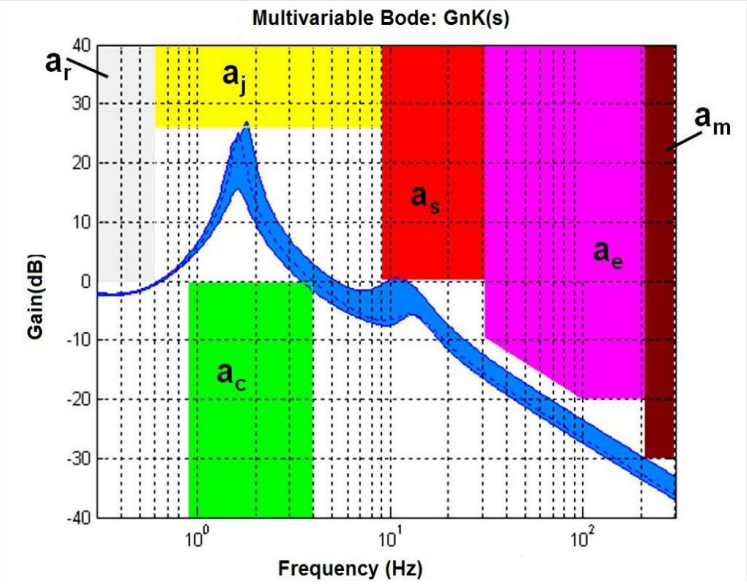

Figure 6: Barriers for Robust Control

The methodology to calculate the matrices **H** and **G** is presented below:

1) The first step is to choose the Gaussian perturbation input matrix, $\mathbf{L}(j\omega)$ and μ, respecting the performance barriers presented in Fig. 6, to fit the FRF of:

$$\frac{1}{\sqrt{\mu}}\sigma_i[\mathbf{C}(j\omega\cdot\mathbf{I}-\mathbf{A})^{-1}\mathbf{L}]$$

2) Calculate the Kalman filter gain matrix $\mathbf{H}(j\omega)$, solving the following Algebraic Riccati Equation (ARE):

$$\mathbf{A}\Sigma+\Sigma\mathbf{A}^{\mathrm{T}}+\mathbf{L}\mathbf{L}^{\mathrm{T}}-\frac{1}{\mu}\Sigma\mathbf{C}^{\mathrm{T}}\mathbf{C}\Sigma=0\Rightarrow\mathbf{H}=\frac{1}{\mu}\Sigma\mathbf{C}^{\mathrm{T}}$$

and verify the Kalman identity using:

$$\mathbf{G_{KF}}(j\omega)=\mathbf{C}\cdot(j\omega\cdot\mathbf{I}-\mathbf{A})^{-1}\cdot\mathbf{H}$$

3) Solve the following ARE, finding **X**:

$$-\mathbf{X}\mathbf{A}-\mathbf{A}^{\mathrm{T}}\mathbf{X}-\mathbf{Q}_3+\mathbf{X}\mathbf{B}\mathbf{R}_2^{-1}\mathbf{B}^{\mathrm{T}}\mathbf{X}=0$$

where

$\mathbf{Q_3}$ is a positive semi-defined given by:

$$\mathbf{Q}_3=\mathbf{Q}_2-\mathbf{N}\cdot\mathbf{R}_2^{-1}\cdot\mathbf{N}^{\mathrm{T}}$$

$$\mathbf{Q}_2=\mathbf{C}^{\mathrm{T}}\cdot\mathbf{Q}\cdot\mathbf{C}$$

$$\mathbf{N}=\mathbf{C}^{\mathrm{T}}\cdot\mathbf{Q}\cdot\mathbf{D}$$

$$\mathbf{R}_2=\mathbf{R}+\mathbf{D}^{\mathrm{T}}\cdot\mathbf{Q}\cdot\mathbf{D}$$

4) Define the controller gain matrix **G** by:

$$\mathbf{G} = \mathbf{R}_2^{-1}(\mathbf{N}^{\mathrm{T}} + \mathbf{B}^{\mathrm{T}} \cdot \mathbf{X})$$

5) It is possible to verify the robustness of stability condition using Fig. 6 and the FRF of :

$$\mathbf{G}_{\mathrm{N}}(j\omega) \cdot \mathbf{K}(j\omega) = [\mathbf{C}(j\omega \cdot \mathbf{I} - \mathbf{A})^{-1}\mathbf{B} + \mathbf{D}] \cdot \mathbf{G} \cdot (j\omega \cdot \mathbf{I} - \mathbf{A} + \mathbf{B} \cdot \mathbf{G} + \mathbf{H} \cdot \mathbf{C} - \mathbf{H} \cdot \mathbf{D} \cdot \mathbf{G})^{-1} \cdot \mathbf{H}$$

The result of the control synthesis is shown in Fig.7 through three FRF for the passive suspension system (thin lines) and the semi-active suspension system (bold lines) in closed loop.

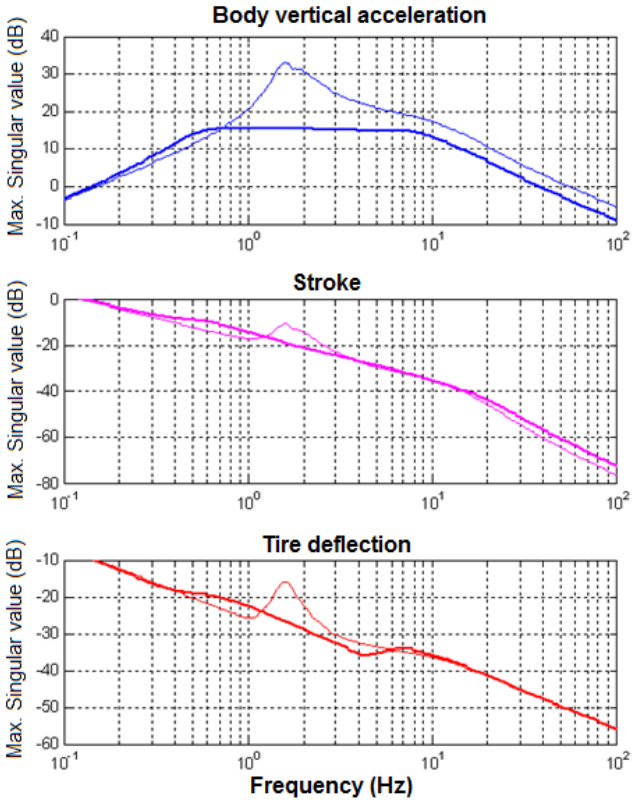

Figure 7. Passive and semi-active system FRF

As shown in Fig. 7, the acceleration amplitude of the vehicle body is significantly reduced along the frequency range of interest, leading to a considerable improvement in vehicle comfort. In the second graph, it can be noticed that there was not a significant increase in the stroke amplitude in low frequencies, which is desired, since in this way shocks are avoided due to suspension course limits. On the other hand, the semi-active closed loop system reduced the wheel hop at 1.8 Hz and avoid the increase of wheel-hop at 10Hz, which can improve the adherence between wheel and ground, with a positive impact in the vehicle handling performance.

4. ELECTRONIC HARDWARE AND SOFTWARE

The electronic hardware consists of:

- four accelerometers sensors assemble in the vehicle body over each wheel,
- four potentiometers installed at each suspension to measure the relative distance between the wheel and the body,
- a digital processor board to read sensors signals, process control algorithm and determine the force at each damper,
- four electric power-drives to generate the electrical currents necessary to activate the dampers force.

The DSP based digital processor board is shown at Fig. 8.

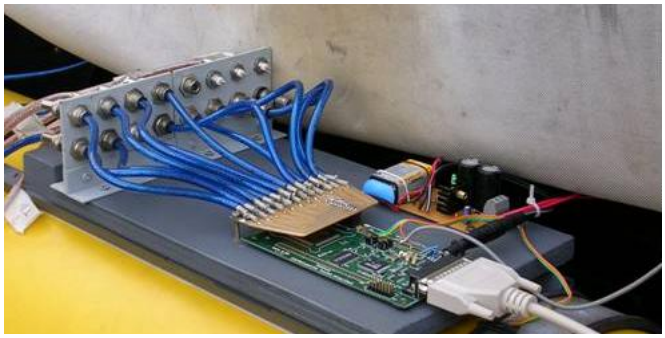

Figure 8. DSP board

It was used the Texas Instruments™ DSP (TMS320F2812) with 150Mips.

The control algorithm software was developed using the Matlab™/Simulink software, where a block diagram of the control was created. Matlab™ can translate the diagrams C language implemented in a Code Composer software (by Texas Instruments™), which translates the program to a DSP machine language and transfer the program to a flash memory at the processor board.

To improve the performance of the semi-active actuators a discrete-time model of each MR damper was used in the control algorithm. This strategy and its benefits are described in Crivellaro (2008), volume 2. The discrete-time model used was described in Crivellaro and Donha (2008).

5. EXPERIMENTAL TESTS

For tests evaluation, six performance indexes were evaluated:

- a_2: the average RMS acceleration of four accelerometers installed in the vehicle body;
- d_{12}: the maximum absolute value of the potentiometers measurement installed between the wheel and the body;
- torsion: index calculated from the sum of the absolute value of the frequency spectra (from 0 to 12.5 Hz) of the PSD curve of the torsion mode of acceleration signal;
- a_z: index calculated from by the sum of the weighted value (according the weighting curve defined in SAE J1490, 1987) of the frequency spectra (from 0 to 12.5 Hz) of the PSD curve of acceleration in ‘z’ direction (vertical) acting over the vehicle driver;
- a_y: index calculated from the sum of the weighted value (according the weighting curve defined in SAE J1490, 1987) of the frequency spectra (from 0 to 12.5 Hz) of the PSD curve of acceleration in ‘y’ direction (transversely) acting over the vehicle driver and
- jerk: the derivative of a_2.

The experimental tests consisted in to drive the vehicle on a plan but irregular terrain in a straight line, along 100 m at 20 km/h approximately. The sensor signals were sampled at 25 Hz rate, in 15 experiments: 10 using the conventional suspension system and 5 using a semi-active suspension system.

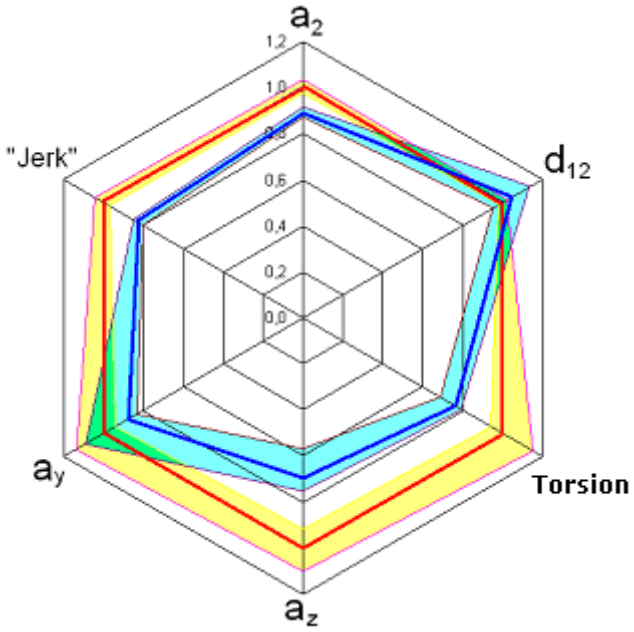

Figure 11. "Radar" graph of index results in the tests

Figure 11 shows the statistical results of experimental tests. The red line shows the conventional suspension system results and the blue line the semi-active system results. Lower values represent better performances for the all six index. The uncertainty margins are showed in yellow area for red curve and light blue area for blue curve. As shows figure 11, except for d_{12}, all other index were improved using semi-active suspension system. Statistically, it is not possible to say that there is a real difference in d_{12} results; anyway it is expected a deterioration in this index.

6. CONCLUSION

As a conclusion, this work could demonstrate the viability of semi-active control systems to pickup truck suspension applications. Semi-active actuators based on magnet-rheological (MR) fluids show a satisfactory performance, although its time response is around 20ms. If the MR shock absorber design is improved to reach a time response of 5 ms, the semi-active system performance will certainly be improved. The main advantage of MR shock absorber is its robustness and durability, when using the most advanced MR fluid available.

The control technique applied could keep the compromise between comfort and tire/road adherence satisfactorily, but this condition limited the semi-active system performance. Performance enhancement could be reached, for example, using adaptive control techniques, since the compromise between comfort and adherence could be relaxed, i.e., the control would focus in comfort when the vehicle is running in a straight line, and focus in the adherence when the vehicle is doing any maneuver.

The next step in this research is to evaluate other form of robust control, as for example, the H∞ approach. Another possible future work is the development of a predictive control of the rear axle based on the behavior of the front axle.

7. ACKNOWLEDGMENTS

The authors would like to express their gratitude to:

- Prof. Dr. Antônio Bombard from UNIFEI, MG, who provided the MR fluid for our experimental tests;
- the Dana Nakata test laboratory team, who was very collaborative and creative in the experimental activities;
- Affinia Automotive Group, in name of Eng. Eduardo Alves and Eng. Hideo Matsuzaki, due to the build of some prototype parts;
- Nuncio Perrella from Texas Instruments, who provide important support in the use of DSP hardware;
- The Dana Brazil employees that directly or indirectly participate in this project.

8. REFERENCES

Crivellaro, C. "**Is semi-active suspension worth being applied in pickup trucks?**" SAE Brasil 2008 International Congress, 2008-36-0220, São Paulo, SP, Brazil, November 2008.

Crivellaro, C.; Santos, E. C. A. dos "**Projeto de um Amortecedor Magneto-reológico**". SAE Brasil 2004 International Congress, 2004-01-3279, São Paulo, SP, Brazil, November 2004.

Crivellaro, C.; Alves, S.; "**Phenomenological Model of a Magneto-rheological Damper for Semi-active Suspension Control Design and Simulation**." SAE2006, November 21-23, São Paulo, SP, 2006.

Crivellaro, C. and Donha, D.C.; "**Discrete-Time Dynamic Model of a Magneto-Rheological Damper for Semi-active Control Design**", ABCM Symposium Series in Mechatronics – Vol. 3 – pp 27-36, 2008.

Crivellaro, C. "**Controle robusto de suspensão semi-ativa para caminhonetes utilizando amortecedores magneto-reológicos**". v1 and v2, 439p., PhD thesis – Escola Politécnica da Universidade de São Paulo, USP. São Paulo, 2008.

Cruz, J.J. da, **Controle Robusto Multivariável**. Edusp Editora da Universidade de São Paulo, São Paulo (SP) Brazil, (in Portuguese), 163 p, 1996.

Crivellaro, C. and Donha, D.C.; "**Performance and Stability Barriers for Robust Control Designs of SUV Active Suspensions**". 18th World Congress of the International Federation of Automatic Control (IFAC), Milano, Italy, 2011a.

Crivellaro, C. and Donha, D. C. "**Fast experimental identification of suspension models for control design**" Proc. IMechE Vol. 225 Part D: J. Automobile Engineering, 2011b.

SAE J1490 Society of Automotive Engineers: **Measurement and presentation of truck ride vibrations**, Warrendale, USA, 1987.

ISO 2631-1 International Organization for Standardization: **Mechanical Vibration and Shock – Evaluation of Human Exposure to Whole – Body Vibration. Part 1: General Requirements.** Geneva, 1997.

Skogestad, S. and Postlethwaite, I. **Multivariable Feedback Control Analysis and Design**. John Wiley and Sons, Chichester, UK, 1996.

9. RESPONSIBILITY NOTICE

The authors are the only responsible for the printed material included in this paper.